JOURNAL OF APPLIED ELECTROCHEMISTRY 7 (1977) 369–378

Electrolytic studies on the system $Ag/Ag_2O/AgO$ in alkaline chloride solutions

J. TURNER

Timex Corporation, Stephenson Industrial Estate, Washington, Tyne and Wear, UK

Received 10 December 1976

Electrolytic silver oxide, formed by the constant current anodization of silver sinters in KOH electrolyte, has been found to be higher in AgO content when prepared in the presence of KCl than when prepared in pure electrolyte. The former AgO is considerably more stable in alkaline solution, seemingly due to the presence of residual AgCl. The formation of unstable oxy-chlorides at potentials more anodic than that for AgO formation results in the isolation of the AgO from the unoxidized Ag in the case of Ag foil electrodes, leading to suppression of the open circuit potential.

1. Introduction

Argentous oxide, Ag_2O, is well known as an electrode material in miniature Zn/alkali button cells; the absolute maximum theoretical energy density of the Zn/Ag_2O system, calculated assuming the two reactants to be non-porous masses without electrolyte, membranes or encapsulation, is 2×10^3 mWh cm^{-3} and the estimated feasible practical energy density for a typical button cell configuration (e.g. I.E.C. R44) would lie in the region of 600–700 mWh cm^{-3}, making it superior in this respect to all conventional systems except Zn/HgO (absolute maximum energy density $2{\cdot}5 \times 10^3$ mWh cm^{-3}) and Zn/AgO ($3{\cdot}3 \times 10^3$ mWh cm^{-3}). Argentic oxide is particularly attractive due to its high volumetric energy density, but it suffers from two disadvantages.

(a) Instability with respect to Ag_2O in alkaline electrolyte, resulting in the reaction:

$$2AgO + 2OH^- \rightarrow Ag_2O + H_2O + O_2$$

(alternatively, reduction of the AgO by organic barrier materials may occur); and

(b) a two-step voltage/time discharge characteristic corresponding to the conversion processes:

$$2AgO + H_2O + 2e^- \rightarrow Ag_2O + 2OH^-;$$

$E^0 = -0{\cdot}570$ V versus SHE

$$Ag_2O + H_2O + 2e^- \rightarrow 2Ag + 2OH^-;$$

$E^0 = -0{\cdot}344$ V versus SHE.

The presence of the first plateau renders the material unsuitable for any application where voltage regulation is of the first importance. For such applications it is desirable for the upper plateau to be completely suppressed at the required discharge current.

The following work arose from attempts to prepare an electrolytic silver oxide, high in AgO content and stable in concentrated sodium hydroxide solution and for which the AgO/Ag_2O discharge plateau was completely suppressed at current densities of the order of 1 mA cm^{-2}.

The ratio of the length of the AgO plateau to that of the Ag_2O plateau has been examined by several authors. Wales and Burbank [1] suggested that the length of the first plateau depended more on the surface area of the charged electrode than on the quantity of AgO. They noted that a low charging rate gave an unusually short AgO/Ag_2O potential region although the total discharge capacity was very large. They attributed this to the formation of larger AgO crystals which presented a smaller surface area/g of AgO and therefore required less Ag_2O to cover them. Similarly, Romanov [2] has reported that mechanical mixtures of AgO and Ag_2O from battery plates gave a shorter first plateau than did the original plates, presumably due to the presence at the current collector of a greater percentage of Ag_2O. Wylie [3] found that the lengths of the two plateaux

Printed in Great Britain. © 1977 *Chapman and Hall Ltd.*

could be equalized in battery plates by putting a highly conductive inert matrix in the electrode. Such observations have been corroborated by Dirkse [4], who demonstrated that for pressed pellets of AgO/Ag_2O the potential of the electrode was that of the material near to the grid, regardless of the composition of the remainder of the pellet. Chapman [5] suggested that charging zinc/silver oxide secondary cells whose electrolyte was saturated with sodium chloride gave a single voltage discharge equivalent to the Ag_2O/Ag level. Positive plates charged in such electrolyte and discharged in chloride-free electrolyte displayed this same property. Less complete suppression has been observed with zincate saturated electrolyte [6].

Several papers [8–11] have examined the influence of current pulse (constant current with superimposed pulse), current interruption, asymmetric a.c. and current reversal on the charge acceptance of silver sinters in potassium hydroxide solutions. These techniques were very successful under certain well-defined conditions (increase in charge acceptance of up to 50%) and this was ascribed to a disruption of the oxide film which allowed penetration of the electrolyte. It was noted that, after charging by an asymmetric a.c. signal with large forward and reverse components, the potential of the initial constant current discharge plateau was lower than that encountered following a charge at the same net current but with smaller components, suggesting that if sufficiently large forward and reverse currents were to be employed the initial plateau would disappear. Such complete suppression has been reported to occur [12]. According to Wales, this phenomenon is related to ohmic losses resulting from an unusually large proportion of the silver being converted to oxide.

The work of Hoar and Dyer [7] suggested that increase in capacity together with voltage suppression might be achieved under the simpler charging conditions of constant current whilst employing Cl^- as electrolyte additive, and it was therefore decided to adopt that approach in the present work. Sintered silver plaques were preferred since these were found to give more reproducible results compared to pressed silver powder compacts. The investigation included fundamental experiments on silver foil with a view to obtaining some insight into the mechanistic influence of Cl^-.

2. Experimental

2.1. *Experiments with silver foil*

The 200 ml capacity three-electrode electrochemical cell used in the experiments with silver foil has already been described [13].

The foil was positioned horizontally, facing upwards, so as to eliminate all but local convection at the electrode surface, and electronic contact was made by means of gold foil through a silicone rubber washer. The electrolyte could be flushed with nitrogen during the course of an experiment.

Cyclic voltammetry was performed on the foil by applying the output from a linear sweep unit to a TR40/3A potentiostat (both Chemical Electronics); i/E curves were recorded on a Bryans 26 000 A4 X–Y plotter. The potentiostat also supplied the constant current for the galvanostatic experiments. The potential of the working electrode (W.E.) with respect to the HgO/HgO reference (R.E.) was monitored as a linear function of time on a Rikandenki B341 potentiometric recorder. For certain experiments, the rest potential of the foil was monitored after charging to oxygen evolution, prior to reverse polarization.

2.2. *Preparations involving sintered silver plaques*

A simple pyrex electrolytic cell, vented to allow the escape of generated hydrogen and oxygen, was employed for the preparative work; two nickel foil (Goodfellow Metals Ltd, 6N) counter electrodes, of the same shape and area, were positioned either side of, and equidistant from, the rectangular sintered plaque. The cell capacity was approximately 500 ml.

2.3. *Experimental preparation*

The silver foil (Goodfellow Metals Ltd, 99·97%, thickness 0·15 mm) was blanked into 1 in ($\sim$ 2·5 cm) diameter discs and degreased in AnalaR acetone (BDH Ltd) prior to incorporation into the cell. The sodium hydroxide and chloride were both BDH AnalaR grade. Triply distilled water was used to make up the various electrolytes containing these reagents.

For the preparative work, BDH AnalaR grade potassium hydroxide and chloride were used and

singly distilled water was employed as the solvent. Sinters were prepared in pyrolytic graphite moulds from 14 g quantities of Johnson-Matthey cypher 120 silver powder (purity 6 N) on expanded nickel (purity 6 N) supplied by Goodfellow Metals; optimum conditions for the sintering process, which was performed in a muffle furnace, were found to be 30 min at 590° C. The latter provided the minimum quantity of residual silver powder over the temperature range 400–1000° C and time 15–120 min studied. The silver powder was heated from ambient temperature and the sinter allowed to cool to below 400° C before removal from the furnace. Sinters prepared in this way were 0·4 cm thick, 7·7 cm long and 3·9 cm wide. An inert atmosphere was not employed, the carbon mould being sufficient to prevent oxidation of the silver.

2.4. *Analytical technique*

Total silver was determined volumetrically using ammonium thiocyanate with ferric alum as indicator, and the free silver by dissolution of the ionic silver in dilute ammonia. Moisture content (< 0·01% by weight) was obtained by heating to 105° C. The relative amounts of AgO, Ag_2O and AgCl were obtained by calculation after heating to 400° C to decompose the oxides and extraction of the residue with dilute ammonia.

2.5. *Gassing tests on silver oxide samples*

Gassing tests were performed on 2 g samples of the various silver oxide samples at 50° C in the apparatus described in an earlier report [13]. The tests, in which a vibrator was employed to dislodge oxygen bubbles from the oxide powder, were conducted over a period of 600 h.

3. Results

3.1. *Cyclic voltammetry on silver foil*

Fig. 1(a) shows a typical cyclic voltammogram obtained in 4 N NaOH. The rest potential of the silver foil was always 0 ± 2 mV with respect to Hg/HgO and the excursion was always commenced at 0 V with respect to Hg/HgO. All potentials quoted therefore correspond to the overpotential of the working electrode.

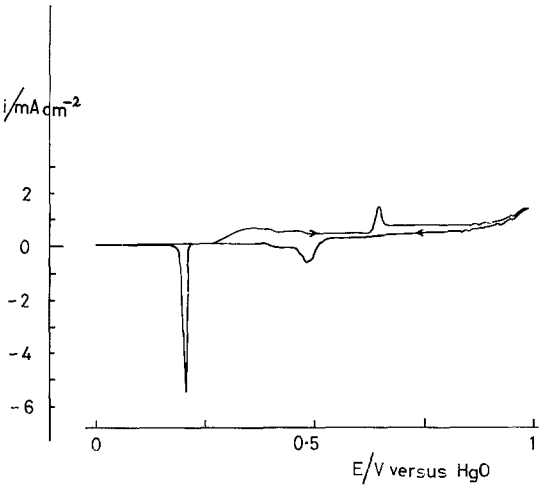

Fig. 1(a). Anodic potential excursion for Ag in 4 N NaOH at ambient temperature, sweep rate 0·83 mV s^{-1}. *Y* axis: i(mA cm^{-2}); *X* axis: η(V).

The influence of the progressive addition of NaCl to the electrolyte can be seen from Figs. 1(b) and (c), and results for the investigation are summarized in Table 1. Several features may be noted: the appearance of a peak due to the oxidation of Ag to AgCl [7]; a marked increase in the degree of oxidation of the foil commencing with chloride formation; the appearance of several anodic peaks in the region where oxidation of Ag^+ occurs, and their progressive shift to more anodic potentials with increase in Cl^- concentration; suppression of the AgO reduction peak,

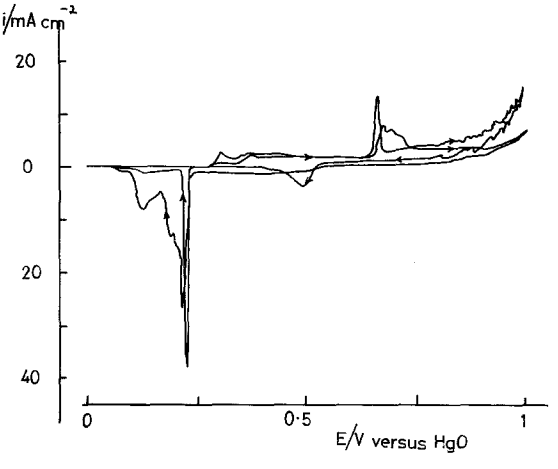

Fig. 1(b). **Anodic** potential excursion for Ag in (a) 4 N NaOH/0·05 M NaCl and (b) 4 N NaOH/0·1 M NaCl at ambient temperature, sweep rate 0·83 m V s^{-1}. *Y* axis: i(mA cm^{-2}); *X* axis: η(V).

Table 1. Oxidation/reduction peak potentials for cyclic voltammetric experiments in 4 N NaOH

Sweep rate ($mV\ s^{-1}$)	*Amount of NaCl* (M)	*Anodic going sweep*				*Return sweep*		
		Ag/AgCl	*Ag_2O*	*Ag_2O/AgO*	*Higher oxides e.g. Ag_2O_3*	*AgO/Ag_2O*	*Ag_2O/Ag*	*AgCl/Ag*
0·83	None	–	372	659	Absent	487	215	–
0·83	0·05	322	375	660	Absent	486	228	140
0·83	0·10	303	360	–	672, 692	Absent	223/192	128
0·83	0·20	282	390	–	692, 726	Absent	180	140
0·83	0·50	256	390	–	762, 792 697, 728 759, 790	Absent	–	63

N.B. All data refer to initial sweeps and potentials are quoted in mV.

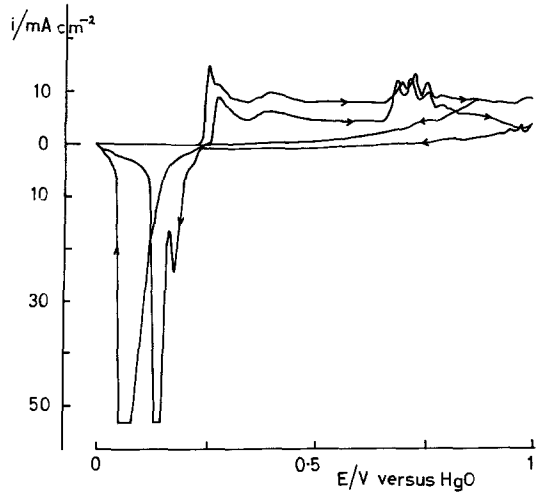

Fig. 1(c). Anodic potential excursion for Ag in (a) 4 N NaOH/0·2 M NaCl and (b) 4 N NaOH/0·5 M NaCl at ambient temperature, sweep rate 0·83 $mV\ s^{-1}$. *Y* axis: $i(mA\ cm^{-2})$; *X* axis: η(V).

and a corresponding decrease in the Ag_2O reduction peak accompanied by a concomitant increase in a peak associated with AgCl, both these peaks being progressively shifted towards less anodic potentials; and an apparent suppression of O_2 evolution.

At higher sweep rates (Fig. 2) an oxidation peak occurred in the return sweep for Cl^--containing electrolytes only. This peak disappeared on allowing the electrode to remain at the anodic extremity of the potential scan for at least 15 s before reversal. The peak shown in Fig. 2 occurred at 683 mV.

Similar behaviour was observed in 7 and 10 N NaOH, although of course higher concentrations of NaCl were needed. For example, Fig. 3 shows the relationship between [NaOH] and [NaCl] for complete suppression of the AgO reduction peak at a sweep rate of 0·83 $mV\ s^{-1}$.

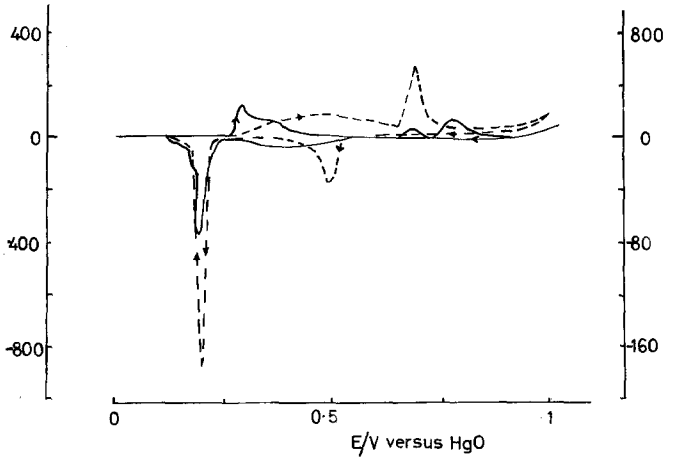

Fig. 2. Anodic potential excursion for Ag in 4 N NaOH and 4 NaOH/0·1 M NaCl at ambient temperature, sweep rate 16·67 $mV\ s^{-1}$. *Y* axis: $i(mA\ cm^{-2})$; *X* axis: η(V).

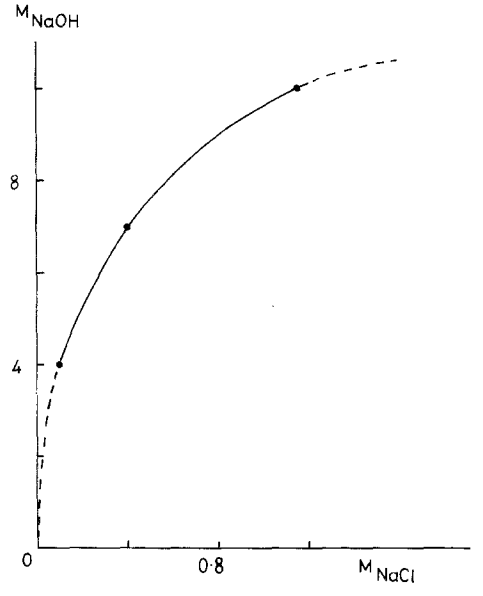

Fig. 3. Plot of minimum concentration of NaCl necessary for AgO/Ag_2O reduction peak suppression at given concentrations of NaOH. *Y* axis: concentration of NaOH (M); *X* axis: concentration of NaCl (M).

3.2. *Galvanostatic polarization of silver foil*

Fig. 4 displays typical charge/discharge profiles, obtained at a current density of 3 mA cm^{-2}, for the progressive increase in Cl^- concentration; the charge/discharge efficiency was approximately 100% in all cases. For Cl^--free electrolyte 26% of the discharge occurred at the AgO level; complete suppression of the latter was achieved at 0·5 M Cl^-, and this pertained even if, after charging, the Cl^--containing electrolyte was changed for 7 N NaOH. The relationship between the degree of oxidation and Cl^- concentration is shown in Fig. 5. Higher levels of addition of Cl^- seemed to cause rupture of the film in the region of AgO/O_2 formation, resulting in the oscillations exhibited in Fig. 6 and increased oxidation of the silver foil. Considerable oxide formation occurred during the oscillatory period of charging, as witnessed by the quantity of charge retrieved on reduction; this oxide formation presumably resulted from direct oxidation of the metallic silver.

3.3. *Potential decay of silver foil on open-circuit*

After galvanostatic charging at 3 mA cm^{-2} to O_2 evolution, electrodes were allowed to stand on

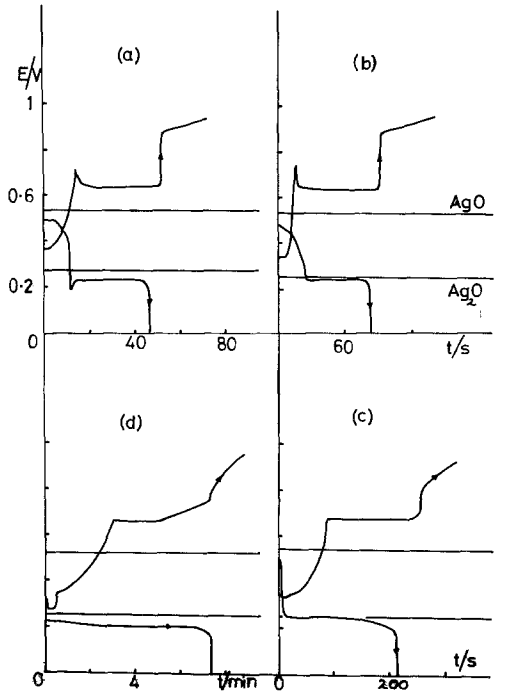

Fig. 4. Anodic/cathodic galvanostatic polarization curves at 3 mA cm^{-2}, ambient temperature. (a) 7 N NaOH; (b) 7 N NaOH/0·2 M NaCl; (c) 7 N NaOH/0·4 M NaCl; (d) 7 N NaOH/0·5 M NaCl. *Y* axis (V); *X* axis (a, b, c) (*t*/s); (d) (*t*/min).

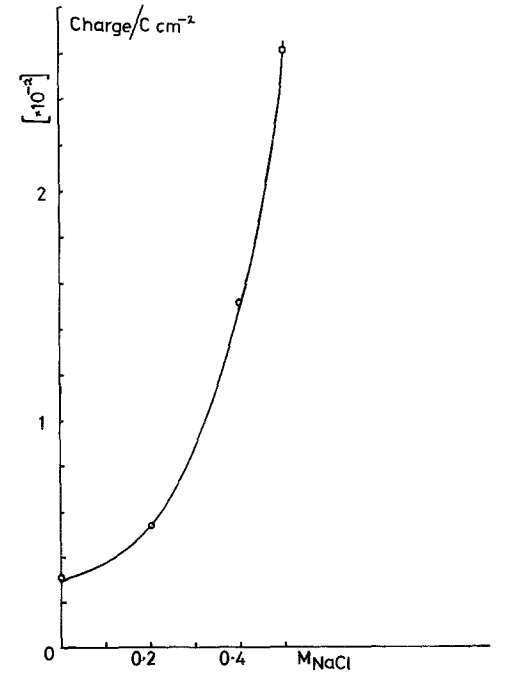

Fig. 5. Plot of degree of oxidation versus sodium chloride concentration for 7 N NaOH. *Y* axis: C cm^{-2}; *X* axis: M_{NaCl}.

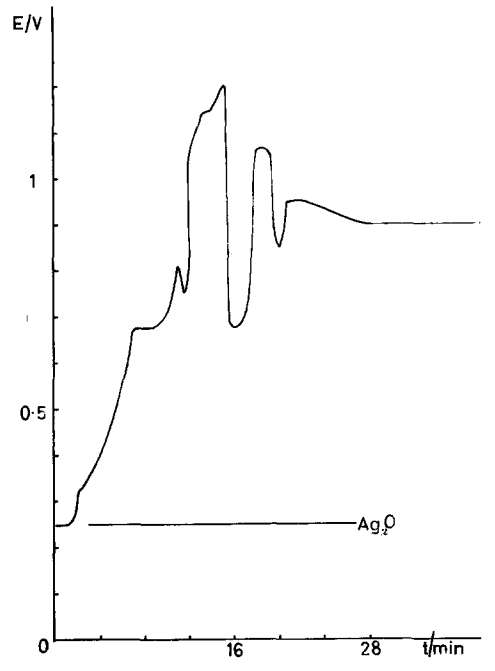

Fig. 6. Galvanostatic polarization curve at 3 mA cm^{-2} ambient temperature for 7 N NaOH/1 M NaCl. *Y* axis: η(V); *X* axis: *t* (min).

open circuit and the potential/time characteristic recorded. Results of these experiments are summarized in Fig. 7, from which it can be seen

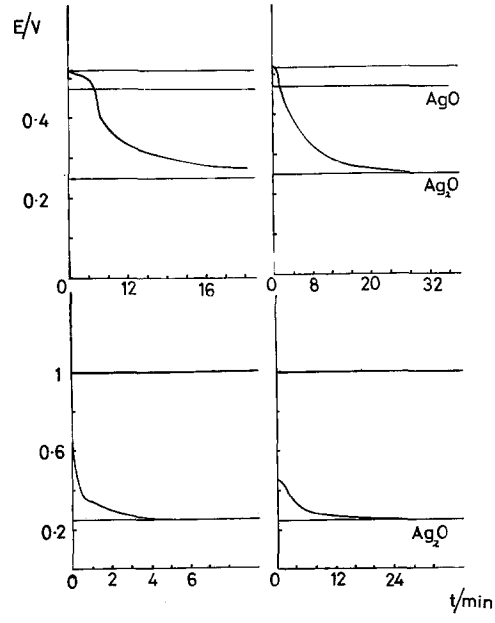

Fig. 7. Rest-potential decay curves after anodization at 3 mA cm^{-2} in: (a) 7 N NaOH; (b) 7 N NaOH/0·5 M NaCl; (c) 7 N NaOH/1 M NaCl; (d) 7 N NaOH/2 M NaCl.

that there was a decay in the potential to that corresponding to Ag_2O. Although complete suppression of the AgO/Ag_2O discharge level at 3 mA cm^{-2} occurred for 0·5 M NaCl, only incomplete suppression of the AgO/Ag_2O open circuit potential occurred even at 2 M NaCl.

The progressive suppression of the AgO/Ag_2O level on open circuit probably corresponded to the increasing presence of $Ag_2O/AgCl$ next to unoxidized silver, the decay itself corresponding to the chemical reaction [14–19].

$$AgO + Ag \rightarrow Ag_2O$$

3.4. *Electrolytic preparation of the oxides of silver*

Preliminary studies established 4·5 N KOH as about the optimum electrolyte concentration for the most efficient constant current charging of the silver sinter. The influence of varying the chloride ion concentration and charging rate is shown in Figs. 8 and 9 respectively, from which it can be seen that the optimum charging rate was *C*/10* and the Cl^- concentration 0·2 M. Further experiments aimed at closer optimization showed 5 N KOH/0·2 M KCl to provide somewhat greater efficiency, giving a composition of 86% AgO, 8·6% Ag_2O, 1·39% AgCl and 3·81% Ag. Charging with current reversal of 25%, 20% and 33·3%

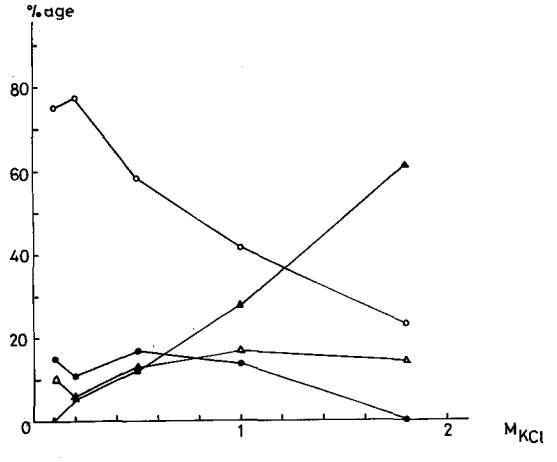

Fig. 8. Composition of electrolytic silver oxide versus molarity KCl for 4·5 N KOH/10 h rate at ambient temperature. *Y* axis: % by weight; *X* axis: M_{KCl}. ○ AgO; ● Ag_2O; △ Ag; ▲ AgCl.

* At the *C*/10 rate, 10 h are theoretically required to convert fully the Ag to AgO, '*C*' referring to that rate at which 1 h is required for complete conversion.

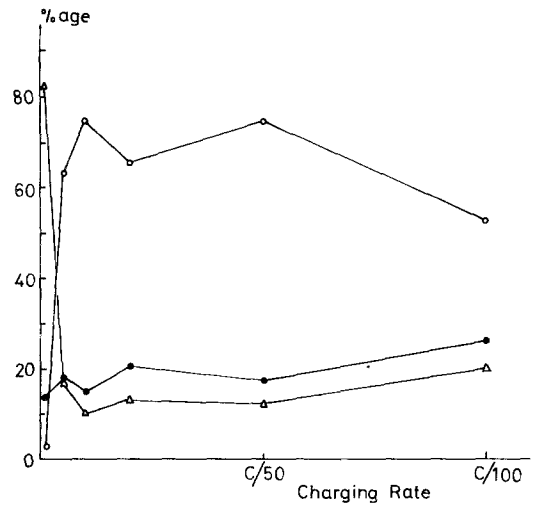

Fig. 9. Composition of electrolytic silver oxide as a function of charging rate for 4·5 N KOH/0·2 M KCl. *Y* axis: % by weight; *X* axis: charge rate/*C*/n. ○ AgO; ● Ag_2O; △ Ag.

(e.g. 25% current reversal, 45 min anodic followed by 15 min cathodic) over 1 h cycle did not significantly improve on this composition; in fact, AgO content was generally lower in such cases (80–85%). The detrimental effect of increasing the Cl^- concentration above ~ 0·2 M does not agree with results obtained on Ag foil, and probably resulted from physical blocking of the pores of the sinter by AgCl, a greater proportion of which with respect to Ag_2O is produced at the higher Cl^- concentrations. It has been calculated using bulk densities that 1 g atom Ag would produce 25·78 cm^3 AgCl compared with 16·22 cm^3 Ag_2O.

The gassing test results of Fig. 10 show the beneficial influence on stability of both charge reversal and residual silver chloride. The samples prepared at *C*/10 constant current and *C*/10 with 20% charge reversal, both with residual AgCl, eventually stopped gassing, whereas the other representative samples (Fig. 10) never stabilized over the time of measurement.

4. Discussion

The various peaks exhibited in the cyclic voltammograms obtained in Cl^--containing electrolyte have been characterized using X-ray diffraction data by Hoar and Dyer [7]. The initial peak is due to the formation of AgCl and the immediate subsequent peaks to Ag_2O; the initial two peaks

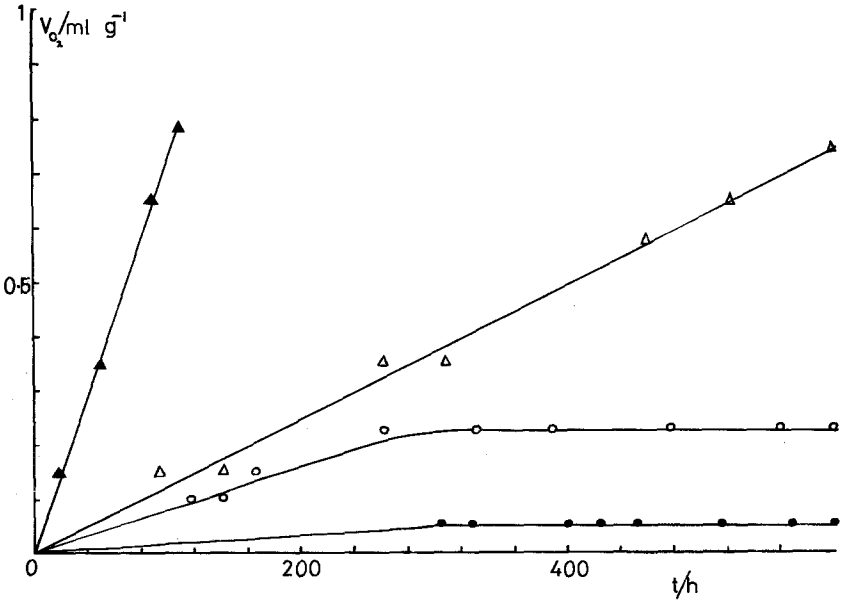

Fig. 10. Selected gassing test results on electrolytic silver oxide. *Y* axis: V_{O_2}/ml g^{-1} oxide; *X* axis: *t* (h).
● 5 N KOH/0·2 M KCl, *C*/10. 20% Current reversal. 82% AgO; 15·5% Ag_2O; 4·2% Ag; 0·70% AgCl.
○ 5 N KOH/0·2 M KCl, *C*/10. 86% AgO; 8·6% Ag_2O; 1·39% AgCl; 3·81% Ag.
△ 5 N KOH, *C*/10. Current reversal. 62·2% AgO; 33·3% Ag_2O; 4·5% Ag.
▲ 5 N KOH, *C*/10. 55·1% AgO; 34·6% Ag_2O; 10·3% Ag.

in the region corresponding to the oxidation Ag(I) → Ag(II) correspond to the formation of AgO. The reduction peaks correspond to the reduction potentials of AgO, Ag_2O and AgCl respectively in the cathodic direction.

The gradual increase in current with voltage for the formation of Ag_2O is consistent with the dissolution–precipitation model of film formation which has been proposed in the literature [20–22], whereas the formation of AgCl, characterized by an immediate rise in current to a maximum, is suggestive of a solid state reaction. The overall increase in degree of oxidation implies a greater porosity of the anodic film formed in the presence of dissolved chloride ion compared to that in pure electrolyte, arising possibly from the greater volume change involved in converting silver to silver chloride compared to Ag_2O (see earlier). An exaggerated form of this can be seen in Fig. 6 in which actual film disruption occurs at high Cl^- concentrations.

As the concentration of Cl^- is increased, Fig. 1(b), a further peak due to the oxidation of AgCl appears. Hoar and Dyer have confirmed that predominantly only AgO is formed in this case, by X-diffraction methods ($\geqslant$ 90% AgO). When the Cl^- concentration is further increased, additional peaks occur and it is postulated that these are due to the formation – by direct oxidation of Ag – of oxy-chlorides such as AgOCl and $AgOCl_2$ which would be expected to form at these potentials [23]. Evidence for this is afforded by the observation of Hoar and Dyer that the peak corresponding to AgCl reduction in the return sweep only appears if Cl^- is present during the oxidation Ag(I) → Ag(II). The oxy-chlorides would decompose to AgCl during the return sweep thus producing the observed peak corresponding to the AgCl reduction potential. The associated suppression of the AgO reduction peak would then result from an AgCl layer at the film/metallic silver interphase effectively isolating the AgO from the unoxidized metal. This might be expected, since it has been shown [24, 25] that AgO formation commences at the Ag_2O/electrolyte interphase, and advances progressively into the film; the *i/E* relationships suggest that oxy-chloride formation occurs subsequent to that of AgO. Examination of the anodic films by addition of 3 N HNO_3 revealed, after dissolution of the superficial silver oxides, a coherent film of insoluble AgCl underneath, which on dissolution of the metallic silver detached itself from the foil. The oxidation peak observed during the return sweep at faster sweep rates as depicted in Fig. 2, which has been ascribed to the oxidation of Ag_2O to AgO [26–28], probably arises in this case from the oxidation,

$$Ag + Cl^- + OH^- \rightarrow AgOCl + H_2O + 2e^-$$

and/or

$$AgOCl + Cl^- \rightarrow AgOCl_2 .$$

The oxidation AgCl → AgO would not be consistent with voltage suppression.

The galvanostatic results reflect the cyclic voltammograms, and in particular demonstrate the excellent charge/discharge efficiency of the system. It can clearly be seen that as the Cl^- concentration is increased, the degree to which the oxidation of Ag to Ag(I) occurs increases. In Fig. 4(d) the AgO oxidation plateau is succeeded by a region of increasing slope probably corresponding to the formation of oxy-chloride, and the discharge plateau is completely suppressed. Table 2 quotes charge/discharge efficiencies after the oxidized foil had been allowed to stand on open circuit for 1 h. It can be seen that oxides produced in the presence of Cl^- are markedly more stable than those produced in the absence of the additive. X-ray diffraction studies showed the crystallographic structure of the former to be identical to that of AgO prepared in Cl^--free electrolyte and identical also to the cubic structure exhibited by AgO prepared by the chemical oxidation of $AgNO_3$ in alkaline persulphate solutions at elevated temperature [29].

Gassing test results on the silver oxide samples prepared from Ag sinters show (Fig. 10) that this increase in stability is due to the presence of residual AgCl; this could be either unoxidized AgCl or chloride arising from decomposition of the oxy-chloride. The decomposition of AgO has been shown to be the result of two concurrent electrochemical component reactions [30, 31]:

$$2AgO + H_2O + 2e^- \rightarrow Ag_2O + 2OH^-$$

$$\frac{2OH^- \rightarrow H_2O + \frac{1}{2}O_2 + 2e^-}{2AgO \rightarrow Ag_2O + \frac{1}{2}O_2}$$

with the overall rate being determined by the

Table 2. Data obtained from galvanostatic polarization experiments at a current density of 3 mA cm^{-2}

Electrolyte composition (for anodic polarization)	*Electrolyte composition (for cathodic polarization)*	*Charge/discharge efficiency (%)*	*Constant discharge potential* (V)
7 M NaOH	7 M NaOH	55	0·23
7 M NaOH	7 M NaOH	73	0·23
7 M NaOH/0·5 M NaCl	7 M NaOH/0·5 M NaCl	84	0·20
7 M NaOH/0·5 M NaCl	7 M NaOH	90	40% at 0·22 60% at 0·19
7 M NaOH/0·5 M NaCl	7 M NaOH	96	58% at 0·214 42% at 0·16
7 M NaOH/1 M NaCl	7 M NaOH/1 M NaCl	100	0·15
7 M NaOH/1 M NaCl	7 M NaOH/1 M NaCl	100	0·17
7 M NaOH/2 M NaCl	7 M NaOH/2 M NaCl	100	0·15

anodic oxygen evolution step. It is therefore likely that the stability afforded by the AgCl arises from its raising the overvoltage for oxygen evolution on the silver oxide/silver system. This explanation is underlined by the observed suppression of O_2 evolution in the presence of Cl^- during the cyclic-voltammetric experiments. Very little oxygen evolution could be observed visually at the anodic extremity of the sweep, in agreement with the i/E relationship. The increase in η_{O_2} would also be a contributory cause of the increased depth of oxidation in the presence of Cl^- additive since the parallel path of oxygen evolution as an alternative to silver conversion would be more difficult.

Button cells (I.E.C. R44) having cathodes of the electrolytic AgO formed in the alkaline chloride electrolyte do not show suppressed open circuit or on-load voltages (across 3 and 6·5 KΩ constant, and 3·3 KΩ pulse loads at 20 and 35° C), but do show excellent shelf-life characteristics even though the AgO is in direct contact with the barrier (semi-permeable) separator. Under these circumstances cells having chemically prepared AgO show poor storage characteristics as can be seen from Table 3, a fact which cannot be entirely explained on the basis of a higher AgO content (> 99%). Electrolytic AgO formed in 5 N KOH at $C/10$ constant rate (AgO content 55%) displays similar poor storage behaviour and barrier degradation. In order to achieve open circuit voltage/on-load voltage suppression the above work indicates that the cathode must be charged *in situ*, so that a layer rich in AgCl isolates the AgO from the cathode can. Voltage suppression could therefore in principle be achieved in secondary systems utilising silver oxide as the cathode.

5. Conclusions

It has been shown that Cl^- additive to the alkaline electrolyte increases the efficiency of oxidation of silver, producing material with a markedly higher AgO content and greater chemical stability in alkaline environments. In the specific case of

Table 3. Results obtained for zinc/silver oxide button cells. Cell dimensions $\phi = 0{\cdot}455$ in, height $= 0{\cdot}220$ in

Cathode composition	*Capacity (to an end point of 1·47 V) After discharge through 6·5 KΩ/35° C* (mA h)		
	After 4 weeks room temperature storage	*After 1 year room temperature storage*	*After 12 weeks storage at 45° C*
Electrolytic AgO (prepared at $C/10$ rate in 5 N KOH/0·2 M KCl)	265	257	231
Chemical AgO (prepared by persulphate oxidation of $AgNO_{3\,aq}$) [29]	255	226	194

secondary silver oxide systems the Cl^- ion could act as a means of suppression of the AgO discharge level, thus achieving good voltage regulation at the sacrifice of specific power.

Acknowledgements

I would like to thank J. R. Moger for his analysis of the silver oxide specimens, and the determination of their stability in alkaline solution.

References

[1] C. P. Wales and J. Burbank, *J. Electrochem. Soc.* **106** (1965) 885.
[2] V. V. Romanov, *Zhur. priklad. Khim.* **33** (1960) 2071.
[3] G. M. Wylie, Investigation of AgO Primary Batteries. Final Report Aug. (1961) AD 267953.
[4] T. P. Dirkse, *J. Electrochem. Soc.* **109** (1962) 173.
[5] C. L. Chapman, Proc. 1st Int. Symp. Batteries (1958).
[6] H. K. Farmery and W. A. Smith, Proc. 3rd Int. Symp. Batteries (1962).
[7] T. P. Hoar and C. K. Dyer, 'Power Sources 3' (Ed. D. H. Collins) (1970).
[8] C. P. Wales, *J. Electrochem. Soc.* **111** (1964) 131.
[9] *Idem*, *ibid* **113** (1966) 757.
[10] *Idem*, *ibid* **115** (1968) 680.
[11] *Idem*, *ibid* **115** (1968) 985.
[12] V. N. Flerov, *Zhur. priklad. Khim.* **37** (1964) 580.
[13] P. F. Hutchison and J. Turner, *J. Electrochem. Soc.* **123** (1976) 183.
[14] B. D. Cohan, J. B. Ockerman, R. F. Amlie and P. Ruetschi, *ibid* **107** (1960) 725.
[15] G. A. Dalin and Z. Stachurski, 'Ageing of Silver-Oxide Zinc Batteries' Extended Abstracts. *Electrochem. Sec. Inc. Battery Division* **8** (1963) 146.
[16] T. P. Dirkse, *J. Electrochem. Soc.* **107** (1960) 859.
[17] C. P. Wales and J. Burbank, *ibid* **106** (1959) 885.
[18] C. P. Wales, *ibid* **109** (1962) 1119.
[19] S. Yoshizawa and Z. Takehara, *J. Electrochem. Soc. Jap.* **31** (1963) 91.
[20] T. P. Dirkse and J. B. De Roos, *Z. phys. Chem. (Frankfurt)* **41** (1964) 1–7.
[21] T. P. Dirkse, D. de Wit and R. Shoemaker, *J. Electrochem. Soc.* **114** (1967) 1196.
[22] M. J. Dignam, H. M. Barrett and G. D. Nagy, *Can. J. Chem.* **47** (1969) 4253.
[23] W. M. Latimer, 'Oxidation Potentials' 2nd Edition Prentice-Hall, New York (1952).
[24] H. R. Thirsk and D. Lax, Ch. 12, 'Zinc-Silver Oxide Batteries' (Eds. A. Fleischer and J. J. Lander) J. Wiley and Sons, Chichester (1971) p. 153.
[25] R. G. Barradas and G. H. Fraser, *Can. J. Chem.* **42** (1964) 2488.
[26] S. Toshima, H. Sasaki and K. Itaya, *Denki Kagaku* **40** (1973) 234.
[27] H. Sasaki and S. Thoshima, *Electrochim Acta* **20** (1975) 201.
[28] T. P. Hoar and C. K. Dyer, *ibid* **17** (1972) 1513.
[29] R. N. Hammer and J. Kleinberg, *Inorg. Synthesis.* **4** (1953) 12.
[30] R. F. Amlie and P. Ruetschi, *J. Electrochem. Soc.* **108** (1961) 813.
[31] P. Reutschi, 'Zinc-Silver Oxide Batteries' Ch. 10. (Eds. A. Fleischer and J. J. Lander) J. Wiley and Sons, Chichester (1971).